Check for updates

Wearable strain sensors: design shapes, fabrication, encapsulation and performance evaluation methods

Nur Nazihah Abu Hassan Zahri,[a] Anis Nurashikin Nordin, [iD] *[a]
Norsinnira Zainul Azlan,[b] Ibrahim Hafizu Hassan,[c] Lun Hao Tung,[d]
Lai Ming Lim[d] and Zambri Samsudin[d]

Highly durable, stretchable, sensitive and biocompatible wearable strain sensors are crucial for healthcare, sports, and robotic applications. While strain sensor designs, fabrication and testing methods have been widely discussed by researchers, not many have discussed sensor improvements *via* implementing designs and protection layers that make the sensor more resilient. This paper will focus on sensor designs (straight line, U-shape, serpentine, and kirigami) and material selection that can provide better performance. Theoretical equations and calculations to indicate how the design shapes contribute to providing better performance are also included. An important aspect which is not often explored is having encapsulation layers which can significantly reduce the formation of cracks when the sensor is subjected to mechanical stress and bending. This review will include post-fabrication steps that are necessary to incorporate protection layers for wearable sensors. Due to the curvilinear shapes of wearable sensors that often need to be in close contact with human skin, reliability and durability testing often differs greatly from that of traditional strain sensors. Recent techniques for performance evaluation specific to wearable sensors such as cyclic stretching, bending, stretch till failure, washability, signal latency, and tensile tests were also discussed in detail. This includes experimental setup and duration of testing and its significance was described. To ensure device safety for the user, biocompatibility assessments need to be made. In this review, cytotoxicity test methods such as trypan blue, cell proliferation and MTT assay were compared and evaluated. By consolidating recent developments, this paper aims to provide researchers and practitioners with a comprehensive understanding of the advancements, and future directions in this rapidly evolving field.

1. Introduction

Strain sensors have been extensively discussed in both industry and academia. With the development of technology, strain sensors have become more accurate, offering more dependable sensing. Strain sensors have been used in various industries such as healthcare, sports, robotics, and communications. Fig. 1 shows the applications of wearable and stretchable strain sensors in those industries. For healthcare applications, human body-induced deformations such as vocal vibration, wrist pulses, muscle twitches and hand gestures can be measured using stretchable and flexible strain sensors.[1–3] Textile-based strain sensors can also be used for sports during lifting exercises, which are capable of measuring joint angles and monitoring sweat.[4–6] Change in sweat volume can be detected when strain sensing fabrics are embedded within super-absorbent hydrogels. These hydrogels swell in the presence of sweat on top of the skin, causing the strain sensor to stretch and produce change in resistance. When used in robotics, strain sensors usually include the use of gloves[7] and a robotic hand or any other prosthetic body part.[8,9] Strain sensors can also be used for communications[10] and have been used to translate sign language.[11]

The advantages of wearable and stretchable strain sensors lie in their conformity with curvilinear surfaces, high mechanical performance, and biocompatibility. When designing strain sensors, it is crucial that the sensor material, fabrication, design, and characteristics meet application specific requirements. Performance metrics for strain sensors placed on the human

[a] Electrical and Computer Engineering Dept., International Islamic University Malaysia, Kuala Lumpur, Malaysia. E-mail: nurnazihah.ahz@gmail.com, anisnn@iium.edu.my

[b] Department of Mechatronics Engineering, International Islamic University Malaysia, Kuala Lumpur, Malaysia. E-mail: sinnira@iium.edu.my

[c] Mechatronics Department, Ahmadu Bello University, Zaria, Nigeria. E-mail: sirhafiz01@gmail.com

[d] Manufacturing Technology and Innovation, Jabil Circuit Sdn. Bhd., Bayan Lepas Industrial Park Phase 4, Penang 11900, Malaysia. E-mail: lunhao_tung@Jabil.com, laiming_lim@Jabil.com, zambrisamsudin@Jabil.com
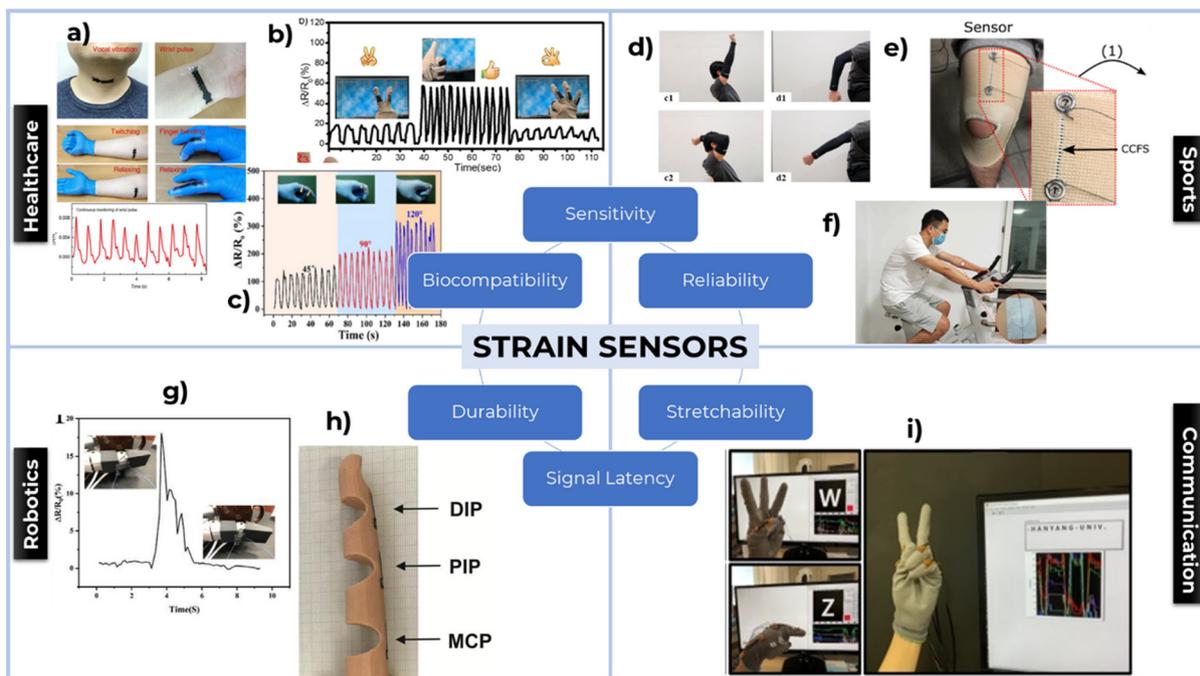
Fig. 1 (a) Measurements of human body induced deformations,[1] (b) finger gesture detection,[2] (c) measurements of different angles of bending finger,[3] (d) classification of training exercise,[4] (e) joint angle detection,[5] (f) sweat monitoring,[6] (g) strain sensing for robot hand,[8] (h) strain sensors on prosthetic finger,[9] (i) sign language translation.[11]

body include stretchability, wearability, durability and ability to produce real-time measurements.

Highly stretchable strain sensors have been successfully fabricated and can withstand a wide range of strain during bending or stretching.[1,12–14] However, currently strain sensors are still not completely wearable as they are less reliable when used repeatedly and often designed to be for single use only. Efforts have been made to improve the reliability and comfortability of these sensors.[15–17] Previous research[3] has reported highly stretchable and wearable strain sensors; however, random cracks may still form during stretching, leading to sensor failure or disconnection. There is not much research that has focused on the role of protective layers in minimizing or reducing the formation of cracks when the sensor is subjected to mechanical stress. Thus, this review paper discusses the usage of protective layers for the strain sensors. Most of the previous reviews also concentrated on the strain sensor material selection and the different types of strain sensor fabrication methods.[18–21] Therefore, this review extends the discussion on post-fabrication steps to include protective layer fabrication.

Previous reviews have also focused on different strain sensor designs such as 3D, geometric, and mechanical structure.[18,22,23] This paper will focus more on the theory and calculations derived from the sensor's design shapes that contribute to better sensor performance. The performance can be analysed by doing characterization tests. These tests include reliability, durability, stretchability, sensitivity, signal latency, and biocompatibility testing of the strain sensor. Almost all previous reviews make comparisons on the strain

sensor's characterization or performance[18–20,24,25] but recent advances in performance evaluation methods for the strain sensor have not been sufficiently covered by the existing reviews.

The basic principle of wearable and stretchable strain sensors relies on converting mechanical deformation resulting from movements of the human body into measurable electrical signals.[26] Mechanical deformation occurs when the material is stretched, creating microcracks and changes in tunnelling resistance between conductive particles during stretching or bending. For this mechanical deformation to occur, stretchable materials such as elastic polymers[27–29] and conductive layers[3,13,30,31] must be used to form the sensor that will convert mechanical strain (microcracks) into electrical signals. Controlled microcrack formation can enhance the performance of strain sensors as it yields a linear relationship between the number of cracks and the change in resistance.[32] Although ultrasensitive, crack-based sensors are highly desirable, these sensors usually cannot withstand large, applied strains, as it leads to sensor cut-off in the conductive pathways.[32] Balance between sensitivity and a viable strain range is still difficult to achieve due to unstable crack structure. To create a high-performance strain sensor, additional factors including the materials, design, encapsulation layer, and fabrication method can be investigated.

Recent research developed a kirigami piezoelectric strain sensor to achieve high sensitivity, durability, and stretchability.[7] The developed sensor was effectively used in a haptic glove for musical instruments. This innovative approach of using kirigami cut patterns in sensor design creates a structure that

can unfold and refold, allowing for greater flexibility and stretchability without compromising the sensor's functionality. Another recent study[33] designed a superhydrophobic strain sensor that can be used for underwater applications such as joint motion detection of a swimmer. This sensor is covered within an encapsulation layer that helps to increase the gauge factor or sensitivity of the sensor. Encapsulated sensors can detect large and small human movements more accurately. The innovative approach of the superhydrophobic strain sensor and extra protection from the encapsulation layer can contribute to signal quality improvement, resulting in more consistent sensor readings in wearable devices.

A high-performance, environmentally friendly strain sensor was developed using graphene/thermoplastic polyurethane (TPU) composite.[34] This sensor demonstrated high sensitivity (GF >3905) with a broad sensing range (0–82.4%), and excellent durability, making it suitable for real-time human motion monitoring. This graphene-based strain sensor was successfully used to monitor joint movements and breathing patterns, indicating its potential in practical applications like wearable health monitoring devices and human–machine interaction systems. The use of polydopamine (PDA) coating[35] enhances the biocompatibility of nitrile butadiene rubber (NBR) and carbon black (CB) strain sensors as it yields a sensor that is safe for human skin. The non-cytotoxic nature of this composite (NBR/CB/PDA) represents a significant advancement in creating skin-friendly sensors, especially for wearable devices.

To summarize, this review will focus on the evaluation methods and experimental setup that can be used to characterize the strain sensor's reliability, durability, stretchability, sensitivity, response and recovery time, and biocompatibility. Different from other reviews, we present a comprehensive review that starts with material selection, fabrication techniques, and the protective layer of the strain sensor. The next section explains the strain sensor design shapes including shape type, design theory, equations, calculations, and performance comparison to find the best design for wearable applications. The following section describes the type of experiments that can be conducted on fabricated sensors to evaluate their performance. Different testing methods such as cyclic stretching test, bending test, stretch until fail test, washability test, signal latency test, and tensile test are discussed. Biocompatibility tests such as cytotoxicity test using different assays such as trypan blue, cell proliferation and MTT assay were compared and evaluated. This comprehensive review describes the strain sensor development from start to finish, encompassing sensor design, fabrication methods and performance evaluation and analysis.

2. Strain sensor fabrication

The fabrication of strain sensors involves multiple processes to ensure accurate and reliable performance, from choosing a suitable material for the application to deciding the method of fabrication. Different ways of fabrication can give different performances of the strain sensors. There are many

methods and materials used in previous studies in fabricating strain sensors. The section below discusses different types of conductive materials and substrates of strain sensors.

2.1. Material selection

Choosing the right materials is important for a strain sensor to exhibit the best performance. The active material is supposed to be conductive to detect electrical changes of the strain sensor. The substrate should be stretchable, wearable, and biocompatible to human skin. A good strain sensor material should possess properties such as high sensitivity, stretchability, durability, and fast response time. Various materials have been explored for strain sensor applications such as carbon based and silver based conductive materials, including graphene/graphite, carbon nanotubes, carbon black, and silver nanowires. Strain sensor substrates such as TPU, PDMS, Ecoflex, elastomer, and paper are also explored. Table 1 provides insights from previous studies on different conductive materials and substrates for strain sensors. Conductive materials such as silver nanowires show a high sensitivity of more than 1000 gauge factor and can stretch up to 50–60% strain which is suitable to detect hand motion. However, its durability lasts only until 200 cycles which is quite low compared to carbon material which can give a durability of 1000 cycles. Silver has a very decent response time of less than 10 ms as the hands need sensors that can detect fast movements. Carbon gives the highest durability of 2000 cycles and lowest response time of 332 ms and is considered as the best candidate for strain sensors. However, its sensitivity is the lowest among all. On the other hand, the sensitivity of graphene strain sensor ranges from 9 to 37 gauge factor. Stretchability, biocompatibility, and conductive material-compatibility are the parameters that can be considered in substrate selection for a strain sensor. Based on a previous study as shown in Table 1, a TPU strain sensor can stretch up to 50–60% which is a suitable range for hand motion detection.

Biocompatible materials ensure that strain sensors are safe for use on the skin without causing irritation or adverse reactions, making them suitable for wearable applications. A previous study[35] produced composite films consisting of nitrile butadiene rubber (NBR) films with the addition of carbon black (CB) and polydopamine (PDA) which were noncytotoxic and highly biocompatible (Fig. 2a). The PDA coating added to the NBR films can improve their biocompatibility, opening the possibility of using coated films in direct skin contact applications Fig. 2c presents a direct attachment of a WDT eutectogel sensor on the skin surface of the abdomen for breath monitoring.[44] Previous work also presented a biocompatible hydrogel strain sensor[45–47] that can be attached to the human skin to detect facial expression and hand motion as shown in Fig. 2b, d and e. Fig. 2f shows that pure silicone can be used to create an insulating and fully biocompatible coating for an on-skin strain sensor.[48] Given that hydrogel has been used mostly

Table 1 Strain sensor materials and performance

| Conductive material	Substrate	Sensitivity (gauge factor)	Stretchability (strain) (%)	Stability/durability (cycle)	Response (time)	Ref.
Silver nanowires	TPU	>1000	50–60	200	<10 ms	36
Carbon nanotube	PDMS	5–9	40	1000	2.5 s	37
Carbon nanotube	Ecoflex	1.75	500	2000	~332 ms	38
Graphene	EPDM/PDMS	20–37	68–120	1000	—	39
Graphene	Polymer hybrid nanocomposite	9–37	>200	>60 000	—	40
Carbon	Elastomer	3.8 ± 0.6	~400	1000	<1 s	41
Carbon paper	PDMS	4.73–25.3	228	1000	0.5 s	42
Carbon black and carboxymethyl cellulose	Paper	4.3	—	1000	240 ms	43
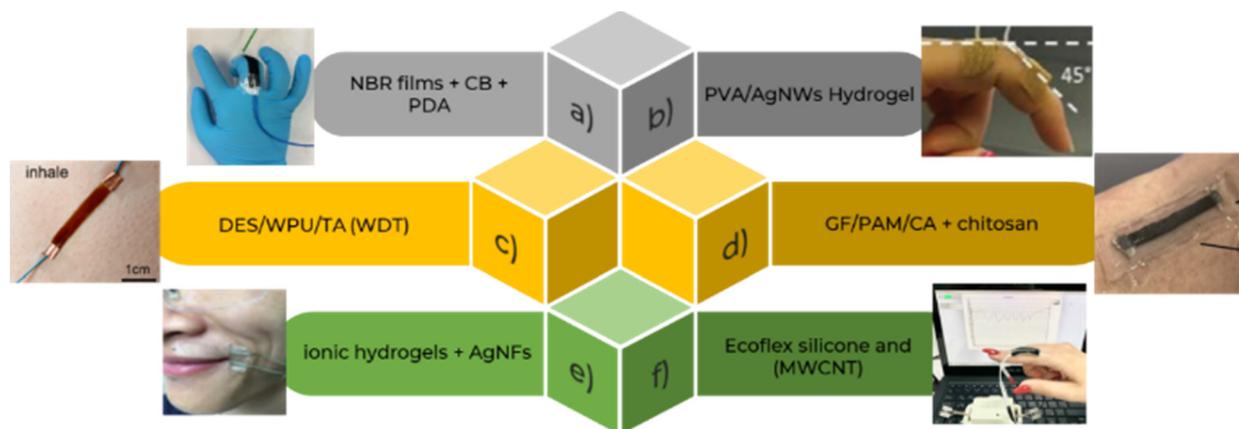
Fig. 2 Biocompatible and wearable strain sensors. (a) Nitrile butadiene rubber (NBR) films with the addition of carbon black (CB) and polydopamine (PDA) strain sensor,[35] (b) polyvinyl alcohol (PVA)//silver nanowires (AgNWs) strain sensor,[45] (c) deep eutectic solvents (DES), waterborne polyurethane (WPU), and tannic acid (TA) (WDT),[44] (d) graphene foam (GF) and polyacrylamide/calcium alginate (PAM/CA) double network hydrogel coupled with chitosan,[49] (e) strain sensor based on a nanocomposite containing ionic hydrogels and silver nanofibers (AgNFs),[47] (f) Ecoflex silicone and multi-walled carbon nanotubes (MWCNTs) strain sensor.[48]

in earlier research, this suggests that it can be an excellent substrate for a biocompatible strain sensor.

2.2. Fabrication technique

There are various methods for fabricating strain sensors, including screen printing, 3D printing, embroidered textiles, and casting techniques. Each of these methods can be useful depending on the application of the strain sensor. Strain sensor fabrication methods shown in Fig. 3 can be used for different applications such as healthcare, infrastructure monitoring, soft robotics, and wearable devices.

Screen-printed (Fig. 3a) sensors are manufactured by printing different types of ink or paste on different substrates. Screen printing is a promising technique due to its low cost, ease of operation, and scalability. Recent studies have shown that screen printing technology can also be used to fabricate strain sensors.[54] This method can be used to print sensors on biocompatible substrates. The development and improvement of screen-printed sensors have made them a promising technique for numerous printed microelectronic applications in industry, including the fabrication of flexible sensors for human health monitoring.[55] Other advantages of screen-printed

sensors include their flexibility of design, reproducibility, and the possibility of modifying the composition of inks to tailor them for specific applications. The process of screen printing contributes to the production of biocompatible sensors suitable for human skin due to their versatility and potential for integrating with flexible and wearable electronics. This method does not involve or introduce any chemical reaction post-printing,[56] making the sensors suitable for human skin. Based on previous studies,[57–61] some of the materials that are suitable for the strain sensor screen printing method are silver nanoparticles, silver nanowires, silver flakes, carbon nanotubes, and carbon graphite.

3D printing (Fig. 3b) is a versatile fabrication method that allows for the creation of complex and customized structures.[51] 3D printing can produce biocompatible sensors using specialized resins and polymers designed for biomedical applications.[62] These materials such as photopolymer-based conductive resins, flexible ultraviolet (UV) resin, and conductive ultraviolet (UV) resin can be custom designed to print sensing prototypes with specific electrical, mechanical, and thermal properties. While 3D printing offers advantages such as high accuracy, repeatability, and customization, it may not achieve the same level of production efficiency as screen printing due to
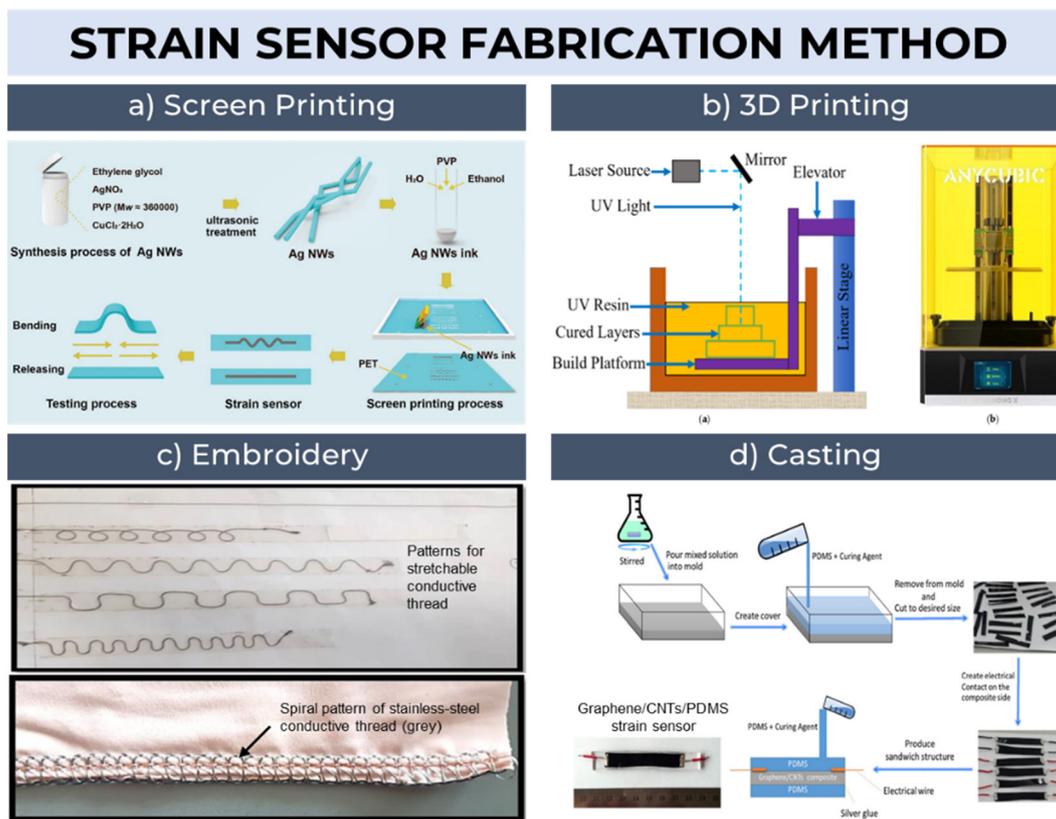
Fig. 3 Fabrication method of strain sensor. (a) Strain sensor screen printing process flow.[50] (b) 3D printing using UV resin material.[51] (c) Embroidery patterns sewn on fabric using conductive thread.[52] (d) Casting process flow of strain sensor.[53]

the complexity of the process and the time-consuming nature of 3D printing.

Embroidered textile (Fig. 3c) refers to a method of creating strain sensors by embroidering conductive threads onto stretchable fabrics such as cotton and polyester. Based on previous study,[63] it provides a flexible and lightweight solution for monitoring human motions and can be seamlessly integrated into various types of clothing. Embroidery can be used with biocompatible substrates to create compliance control stitch patterns in the substrate materials.[52] The casting method process (Fig. 3d) involves pouring material into a mold to create solid objects such as strain sensor. It is highly suitable for the fabrication of strain sensors on a large scale[64] and for designing three-dimensional structures. Strain sensors created through casting are susceptible to errors and interferences, such as changes in resistance due to temperature or humidity, hysteresis, creep, or fatigue, which can reduce accuracy and repeatability. On the other hand, screen printing provides a more precise and controlled way to apply conductive materials onto substrates, offering better accuracy and reliability in strain sensing applications.

Different fabrication techniques such as screen-printing, 3d printing, embroidery and casting method have different benefits in terms of material compatibility, scalability, and precision. Stretchability, durability, and sensitivity are just a few of the sensor characteristics that are impacted by the

fabrication method selection. New manufacturing techniques are evolving as technology progresses, offering increasingly more advanced and effective ways to produce sensors.

2.3. Encapsulation techniques

Encapsulation of strain sensors is one of the important aspects for sensor performance. Protective layers can enhance the durability, accuracy, and lifespan of sensors by protecting them from mechanical factors such as cracks and sensor cut-off and environmental factors, such as moisture, dust, and chemicals. It is also important to select the right encapsulation layer based on the specific application and environmental conditions. Different types of protective coatings are introduced. Fig. 4a and d shows the use of PDMS as the protective layer of strain sensors. The dip-coating technique[65,66] was used to encapsulate the strain sensor within thin PDMS. The PDMS sheath helps to maintain the sensor's structural integrity, preventing the sensor from peeling off during repeated stretching or bending. The use of this PDMS coating improves the sensitivity of the PU yarn-based strain sensor from 18.33 to 661.59 and still maintained its original electromechanical properties during 10 000 stretching/releasing cycles. This qualifies the sensor for longer-term usage. The PDMS coating also makes the sensor waterproof, protecting the sensing layer from moisture and making the sensor less sensitive to humid
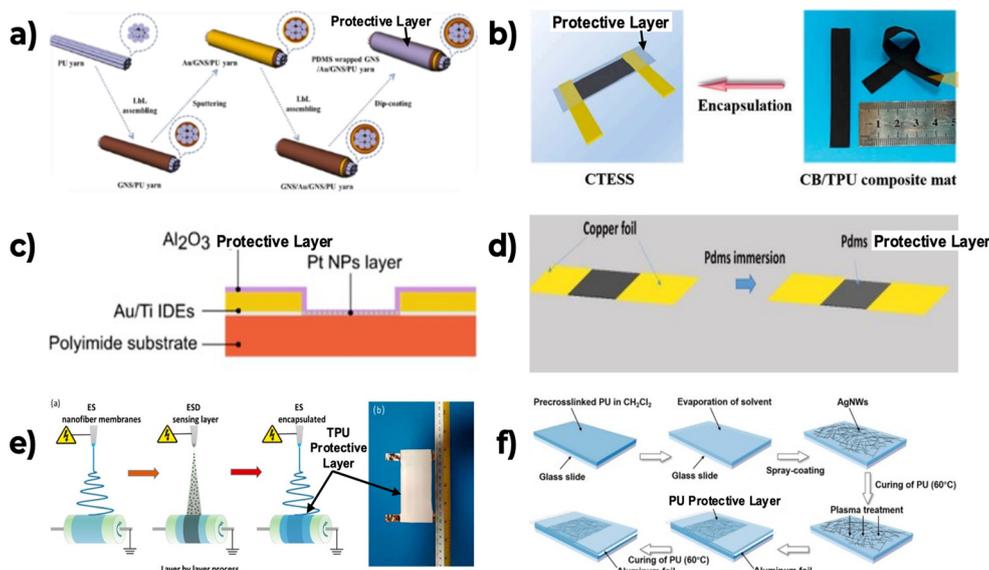
Fig. 4 Examples of protective encapsulation layers. (a) PDMS-wrapped GNS/Au/GNS/PU yarn,[65] (b) CB/TPU/Ecoflex strain sensor (CTESS),[67] (c) alumina as protective layer,[68] (d) PDMS-encapsulated MXene@polyester fabric strain sensor,[66] (e) stretchable MXene/thermoplastic polyurethane-based strain sensor,[69] (f) PU as protective layer of the sandwich structured PU/AgNW/PU composite strain sensor.[70]

environments. The flexible and stretchable nature of PDMS allows the protective layer to conform and deform along with the sensor without cracking or losing its protective properties.

CB/TPU/Ecoflex strain sensor (CTESS) (Fig. 4b) was fabricated by encapsulating the CB/TPU composite mat with Ecoflex to secure the conductive network. Ecoflex is absorbed into the TPU fiber network during the encapsulation process, and it wraps the CB/TPU fiber to form a sandwich-like structure. The conductive network of CB/TPU fibers is effectively shielded by the self-formed sandwich structure, allowing it to provide more consistent and reliable readings over time and under various conditions.

There is also a previous work[68] that used alumina to encapsulate the sensor. The alumina protective coating is deposited on top of a strain sensor (Fig. 4c) using an atomic layer deposition (ALD) system. This technique allows more precise control of the coating thickness and uniformity and can be used for the application of very thin layers of alumina. This is advantageous as it protects without significantly altering the sensor's overall dimensions or flexibility. Alumina can also act as a protective coating against humidity while in adverse conditions such as variations in relative humidity and repeated mechanical stress. Utilizing alumina as a protective coating is an inventive way to improve reliability and resilience to environmental stresses in strain sensors. This is useful for applications where sensors must function in difficult or unpredictable situations, including outdoor spaces where mechanical stress and humidity are frequent occurrences.

One example of a TPU encapsulated strain sensor is the MXene/thermoplastic polyurethane based strain sensor (Fig. 4e) developed by Fang et al.[69] This sensor was fabricated using a combined electrospinning and micromachining process, resulting in a highly stretchable and sensitive strain

sensor with a wide sensing range. The high elasticity property of TPU is also crucial for uniform strain distribution, and also increases the operating range of the strain sensor.[69] After the sensor is stretched, microcracks can be seen on the fiber, but most of them can still maintain a good connection state. The TPU encapsulation in this case not only protected the strain sensor from external factors but also contributed to the sensor's overall performance by enhancing its stability and sensitivity.

Another example (Fig. 4f) is when a solution of a pre-crosslinked polyurethane in dichloromethane is poured onto the surface of AgNWs forming a protective layer; the former penetrated into the interconnected pores of the AgNW network due to the strong affinity between the imino groups of PU and the surfaces of AgNWs. Encapsulation of the conductive networks allow the sensor to be highly sensitive and protected from damage induced by limited deformation.[70]

The choice of protective layer for a strain sensor depends on the specific application and requirements. Ecoflex and PDMS are suitable for wearable and medical applications due to their high flexibility and biocompatibility, while TPU is suitable for thermal management applications due to its high thermal conductivity and bending performance. The use of TPU in strain sensors offers benefits such as high stretchability, sensitivity, and stability, making it a viable option for various sensing applications, especially those requiring flexibility and durability. Alumina is suitable for protecting strain sensors from humidity and corrosion due to its high thermal conductivity and resistance to humidity and corrosion.

Protective layers are crucial for enhancing sensor durability, water resistance, and overall performance. Materials like PDMS, Ecoflex, and alumina coatings have shown significant promise

in protecting sensors while maintaining their flexibility and sensitivity. The encapsulation process not only shields the sensor from environmental factors but can also contribute to improved strain distribution and sensor stability. As wearable technology advances, the development of more effective and biocompatible encapsulation methods remains a key area of research.

3. Strain sensor design shapes

When designing strain sensors with different shapes, there are several factors to consider. These factors include sensitivity, flexibility, durability, ease of fabrication, and optimal sensor placement. The strain sensor should be able to detect small changes in strain accurately. The shape of the sensor can affect its sensitivity, with some designs being more sensitive than others. In terms of flexibility, the sensor should be able to conform to the shape of the object it is measuring strain. This is especially important for applications where the object is subject to bending or twisting. The sensor should be able to withstand the conditions it will be exposed to, such as temperature changes, moisture, and mechanical stress. The design of the sensor can affect its durability, with some shapes being more robust than others. The sensor should also be easy to manufacture, preferably using low-cost and scalable techniques. The design of the sensor can affect its manufacturability, with some shapes being more suitable for mass production than others. In some applications, the placement of the strain sensors on the object can affect their performance. Researchers have developed optimization methods to determine the best sensor placement for specific structures. The design of the sensor should consider these optimization methods to ensure accurate and reliable measurements.

There are many different designs and configurations of strain sensors used in research and industry such as straight line, serpentine, U-shape, and kirigami. Each design has its own unique properties and advantages for different applications. The choice of design will depend on factors such as the specific application, material properties, and desired sensitivity and range of motion. The differences between straight line, U-shape, serpentine, and kirigami strain sensors lie in their structural designs and mechanical responses to strain.

Straight line (Fig. 5a and b) strain sensors[71] typically exhibit a linear response to strain and are suitable for basic strain measurement applications, although they have limited stretchability and flexibility compared to more complex designs. U-shape strain sensors (Fig. 5c and d) offer improved stretchability and flexibility due to their curved structure, providing enhanced sensitivity and durability for moderate strain measurement applications.[72] Serpentine strain sensors (Fig. 5g and h) feature a meandering, sinusoidal shape[73] that allows for significant stretchability and flexibility, making them
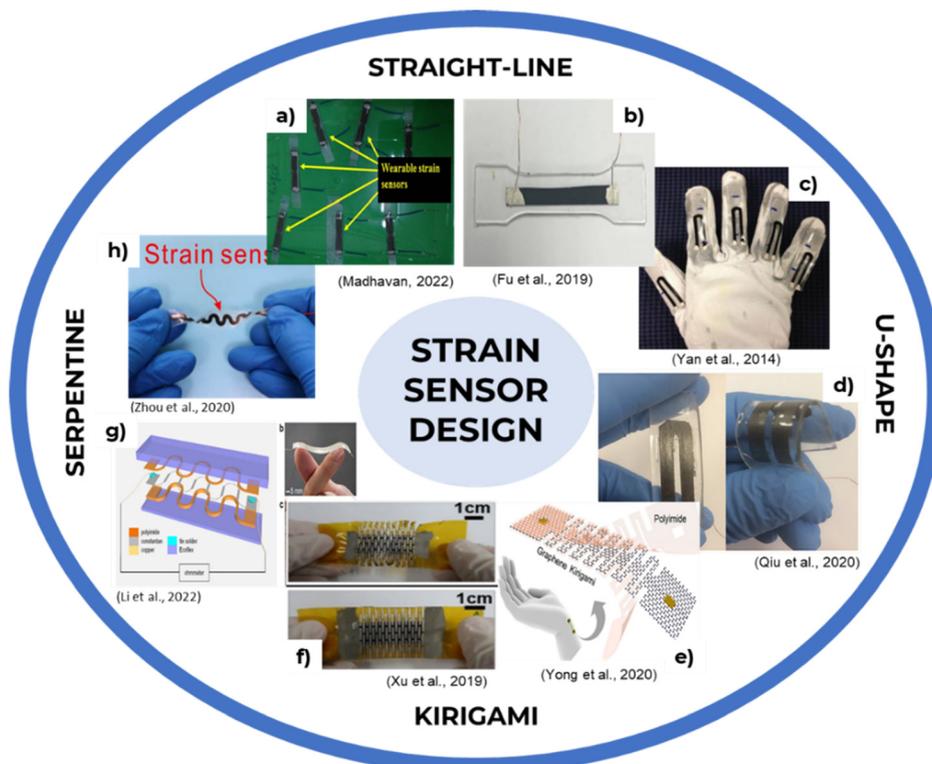

Fig. 5 Strain sensor design and shape. (a and b) Straight line strain sensor,[37,71] (c and d) U-shape strain sensor,[72,74] (e and f) kirigami strain sensor,[47,75] (g and h) serpentine strain sensor.[73,76]
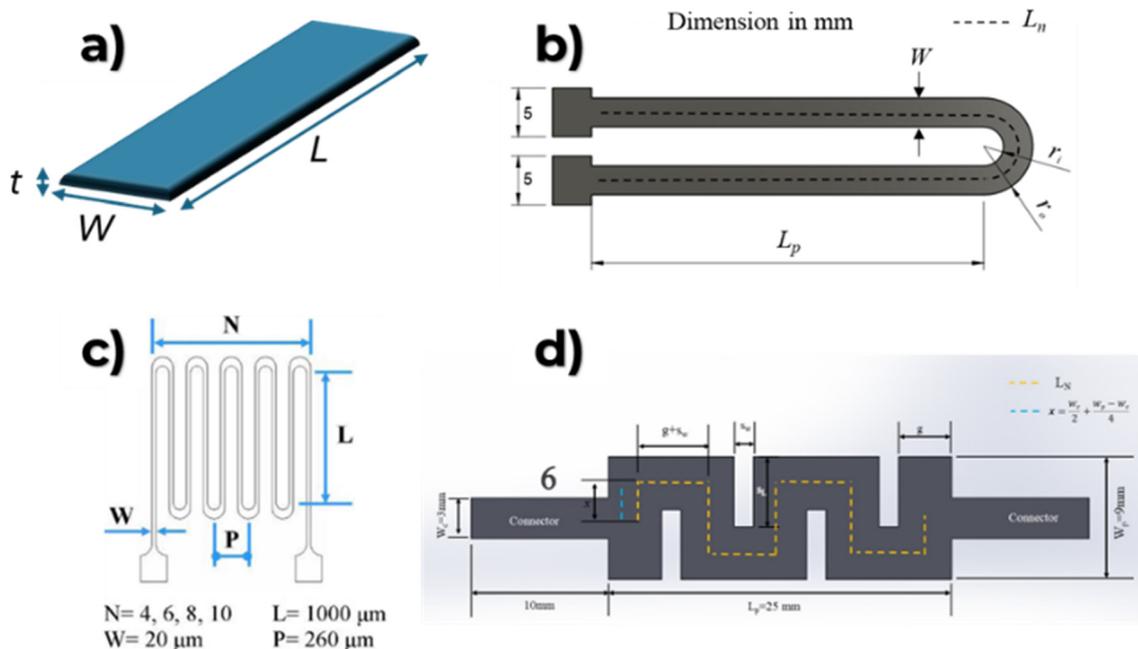
Fig. 6 Strain sensor design shape parameter and dimension. (a) Straight line, (b) U-shape, (c) serpentine, (d) kirigami.

suitable for wearable and stretchable electronics. Kirigami strain sensors (Fig. 5e and f) utilize a design inspired by the Japanese art of kirigami, involving the strategic introduction of cuts and patterns[40] to enhance stretchability and conformability, offering exceptional adaptability to various surface geometries and high mechanical compliance for advanced applications. These different designs cater to specific requirements in strain sensing, offering varying levels of stretchability, flexibility, and sensitivity, with the choice of sensor design depending on the specific application and the mechanical demands of the intended usage. Fig. 6 shows the shape parameters and dimensions of the strain sensors.

3.1. Straight line

The straight line design as shown in Fig. 6a is a simple configuration where the sensing element, such as a resistive film, is arranged in a straight line along the direction of the applied force or deformation. The deformation or strain of the material can be quantitatively and directly measured using eqn (1).

The strain sensor serves as a mechanical-to-electrical converter by converting the mechanical strain into a change in electrical resistance. It produces a voltage change proportionate to the strain because of this change in resistance.

The equation of strain is given by,

$$\varepsilon = \frac{\Delta L}{L} \tag{1}$$

where ε is the strain, L denotes the material's length, and ΔL is the change in length due to external force.

Hooke's law states that the amount of deformation (strain) in an object is directly proportional to the force (stress)

applied to it if the deformation remains within the elastic limit of the material. Mathematically, it can be expressed as:

$$\sigma = \varepsilon \cdot E \tag{2}$$

where σ represents stress, ε represents strain, and E is the modulus of elasticity, *i.e.* Young's modulus.

In the context of electrical strain gauges, which are commonly used to measure strain, the change in the electrical resistance of the gauge is proportional to the strain experienced by the material.

Mathematically, the relationship between resistance and strain can be expressed as follows:

$$GF = \frac{\left(\dfrac{\Delta R}{R_o}\right)}{\varepsilon} \tag{3}$$

where ΔR is the change in resistance, R_o is the initial resistance of unstretched sensor, GF is the gauge factor, and ε is the strain experienced by the material.

Resistivity is a property of a material that affects its resistance, and strain is a measure of the deformation of a material that can be related to changes in its resistance. The relationship between resistivity, resistance, and strain is fundamental to the operation of electrical strain gauges.

The relation between resistivity and resistance is expressed as:

$$R = \rho \frac{L}{A} \tag{4}$$

where ρ is the resistivity, L is the length of the conductor, and A is the cross-sectional area.

To calculate the strain using a straight line strain sensor, the sensor is typically placed on the surface of the material in the direction of the expected deformation. When it stretches, the distance between two points on the sensor changes, causing a change in the electrical resistance of the sensor. For example, a straight line strain sensor that is 10 cm long is placed on a material that is expected to stretch by 1 cm. The change in length of the sensor, ΔL, would be 1 cm, and the original length of the sensor, L_o, would be 10 cm.

Using eqn (1), we can calculate the strain as:

$$\varepsilon = \frac{\Delta L}{L_o} = 1 \text{ cm}/10 \text{ cm} = 0.1 \text{ or } 10\%$$

This means that the material has stretched by 10% along the direction of the sensor.

The resistance was calculated using eqn (4) according to the resistivity of the material used and the gauge factor (GF) was calculated using eqn (3). For example, the resistance was calculated as in Table 2 by using the resistivity 2.1427 Ω m of the C/TPU/Tegaderm from previous work.[77] Using the thickness of the sensor of 0.0001 m and width of 0.01 m, the area is 0.001 m. The gauge factor of the straight line design is 0.9986 as shown in Table 2.

Another research has developed a straight line strain sensor using a multi-wall carbon nanotube (MWCNT)/polydimethylsiloxane (PDMS) composite.[37] The composite with 7% MWCNTs was found to be the most effective in terms of strain sensing compared to those with 5% and 9% MWCNTs. The strain sensor showed a gauge factor of 5–9 under 10–40% strain, with a linear curve of relative change in resistance *versus* strain. Furthermore, the strain sensor exhibited a quick response time, low hysteresis, and great stability under 1000 cycles of stretching and releasing, demonstrating excellent long-term endurance to mechanical stimuli. The strain sensor was successfully utilized to monitor human finger and wrist bending, precisely sensing motion deformation and states.

3.2. U-shape

A U-shape strain sensor is another configuration where the sensing element is arranged in a U-shape, which allows for greater sensitivity and range of motion. Fig. 6b shows the U-shape design of the strain sensor.

The strain of a U-shape strain sensor can be calculated using the following equation:

$$\varepsilon = \frac{\Delta L}{L_p} \tag{5}$$

where ε is the strain, L_p denotes the material's length, and ΔL is the change in length due to stretching of the U-shape sensor

Length L_n is the length from the start of the connector to the end of another connector. L_n is useful in calculating the resistance of a U-shape strain sensor using eqn (4) before and after strain is applied. Length L_n is calculated using the following equation:

$$L_n = L_p \times 2 + \pi \left(\frac{r_o - r_i}{2} + r_i \right) \tag{6}$$

Assuming that the U-shape design has 0.001 m width, thickness of 0.0001 m, r_o of 0.003 m, r_i of 0.002 m, L_p of 0.04 m, and L_n of 0.1 m, the resistance can be calculated as shown in Table 3. The U-shape design allows easy connection at the end of the connector. A recent study developed a U-shape stretchable elastomer/graphene strain sensor that can measure strain with high resolution up to 0.089% and accuracy of over 99.7%. The resolution refers to the minimum dimension of accurate measurement.[39]

3.3. Serpentine

The serpentine design (Fig. 6c) in strain sensors involves a pattern that resembles a series of connected waves or curves, resembling the shape of a snake or a serpentine path. The serpentine-shaped film structure allows for increased flexibility, stretchability, and excellent tortuosity of the sensor and illustrates the application capability in skin-mountable wearable electronics, human-machine interactions, and soft robotics.[78] The total length of the wires will affect the amount of resistance. The longer the wire, the higher the resistance that there will be. Thus, this design will allows higher resistance within a smaller area. Applying a tensile strain to the substrates causes separation of the serpentine traces, increasing the resistance while using a smaller area.[79]

The serpentine design helps the sensor to accommodate the deformation or stretching of the material it is attached to without affecting its performance or accuracy. The wave-like structure allows for better distribution of strain across the sensor, reducing the chances of localized stress concentration that could lead to sensor failure. Researchers present a novel flexible strain sensor in serpentine design as shown in Fig. 6c.[80] Their results demonstrated that the gauge factor is large when the line width of the serpentine pattern of SWCNNs is small.

3.4. Kirigami

Kirigami strain sensor is a type of flexible strain sensor that is inspired by the Japanese paper-cutting art of kirigami as shown in Fig. 6d. In this design, a thin and flexible substrate, such as a polymer film, is patterned with cuts that create a flexible lattice structure. The lattice structure can undergo large strains while still maintaining its electrical conductivity.

Table 2 Resistance of straight line strain sensor

Design	Material	Resistivity (Ω m)	L_o (m)	R at 0% (kΩ)	R at 10% (kΩ)	ΔR (kΩ)	GF
Straight line	C/TPU/Tegaderm	2.1427 (ref. 77)	0.1	214.3	235.7	21.4	0.9986

Table 3 Resistance of U-shape sensor

Design	Material	Resistivity (Ω m)	L_p (m)	L_n	R at 0% (kΩ)	R at 10% (kΩ)	ΔR (kΩ)	GF (k)
U-shape	C/TPU/Tegaderm	2.1427 (ref. 77)	0.04	0.1	1882.45	2053.86	171.42	0.9106

To use a kirigami strain sensor as a strain gauge, electrically conductive material is deposited on the substrate, filling the cuts, and creating a continuous electrical pathway. When the substrate is subjected to a strain, the lattice structure deforms, causing a change in the electrical resistance of the material. This change in resistance can be measured and used to calculate the strain experienced by the material.

One of the key advantages of a kirigami strain sensor is its stretchability. Based on previous work, kirigami design is proven to exhibit strain-insensitive electrical properties of up to 240% applied tensile strain, including a combination of stretching, twisting, and/or shearing.[81] This shows that kirigami design allows for better elongation compared to straight line and U-shape strain sensors.

Taking resistivity from previous experimental work,[77] the gauge factor of kirigami design can be calculated as shown in Table 4, which is 0.5542.

For comparative analysis, as shown in Table 5, straight line designs are best for simple, precise measurements but lack flexibility for complex applications. U-shape designs offer a balance between simplicity and improved flexibility, suitable for moderate strain applications. Serpentine designs excel in stretchability and flexibility, making them ideal for wearable and soft robotic applications. Kirigami designs offer the highest stretchability and adaptability, suitable for the most demanding flexible electronic applications. The choice of design depends on the specific application requirements, balancing factors such as required strain range, flexibility, ease of manufacturing, and the complexity of the surface or movement being measured.

A comparison of different strain sensor shape designs and their performance, such as sensitivity, stretchability, stability, and signal latency are summarized in Table 6. The Kirigami design appears to have a good overall performance, with high stability, good stretchability, and fast signal response time. Stability is an important factor in the performance of strain sensors, as it

Table 4 Resistance of Kirigami design

Design	Material	Resistivity (Ω m)	ΔL at 10% strain (m)	R at 0% strain (kΩ)	R at 10% strain (kΩ)	GF
Kirigami	C/TPU/Tegaderm	2.1427 (ref. 77)	0.027	249.17	262.98	0.5542

Table 5 Comparative analysis of different strain sensor shapes

Design shape	Pros	Cons	Suitable applications	Ref.
Straight line	- Simple design - Linear response to strain - Suitable for basic strain measurement - Easy to fabricate	- Limited stretchability and flexibility - May not conform well to complex surfaces	- Structural health monitoring - Precise strain measurements in rigid structures	37 and 71
U-shape	- Improved stretchability compared to straight line - Enhanced flexibility - Better sensitivity for moderate strain - Allows easy connection at ends	- Limited to be stretched in one axis for the highest performance	- Sensors for prosthetic limbs requiring extreme flexibility - Applications requiring easy electrical connections - A long flexible curve surface	74 and 72
Serpentine	- High stretchability and excellent flexibility - Better distribution of strain - Can accommodate large deformation - Higher resistance in a smaller area	- More complex design and requires more precise manufacturing	- Skin-mountable wearable electronics - Applications requiring high stretchability	73 and 76
Kirigami	- High stretchability - High adaptability to various surface geometries - Maintains electrical conductivity under large strains - Combines stretching, twisting, and shearing capabilities	- Complex design and manufacturing process - May require specialized cutting techniques	- Advanced wearable devices - Sensors for prosthetic limbs requiring extreme flexibility - Highly stretchable electronic skin for robotics - Strain measurement on non-planar or irregularly shaped surfaces	47 and 75

Table 6 Comparison of strain sensor performance for different shape designs

Shape design	Material	Sensitivity	Stability	Stretchability	Signal latency	Ref.
Straight line	MWCNT/PDMS	GF 5–9	1000 cycles	Under 10–40% strain	<5 s response time	37
Straight line	Hydrogel	GF 3.83	100 cycles	Of 10% strain	<2.5 s response time	31
Straight line	CNT–Ecoflex	GF 1.75	>2000 cycles	500% strain	~332 ms response time	38
Serpentine	GNPs/MWCNTs/SR	GF 6.3–2675.5	>2000 cycles	100% strain	~46 ms response time	78
U-shape	EPDM/graphene, PDMS/graphene	GF 20–37	1000 cycles	120% (EPDM/graphene), 68% (PDMS/graphene)	0.16 s (PDMS/graphene) 0.18 s (EPDM/graphene)	39
Kirigami	Graphene–polymer hybrid nanocomposite	>80% delta R at 60% strain	>60 000 cycles	>200% strain	<1 s response time	40
U-shape	Carbon/elastomer	GF 3.8 ± 0.6	1000 cycles	~400%	~1 s response time	41

ensures that the sensor maintains its accuracy and reliability over time and under different environmental conditions.

The kirigami design appears to be the most stable of the designs, indicating that it is less likely to degrade or lose performance over time or in response to external factors such as temperature or humidity. Stretchability is another key factor in the design of strain sensors, particularly for applications where the sensor may need to conform to irregular or curved surfaces or be subjected to bending or stretching. The kirigami design appears to have good stretchability, suggesting that it can bend and flex without losing its sensitivity or accuracy. In applications such as hand gesture detection, where rapid movements and response times are important, a fast signal latency is critical. The kirigami design appears to have a fast response time, making it well suited for such applications.

4. Strain sensor performance evaluation method

Evaluating the performance of strain sensors is essential to ensure their accuracy, reliability, and functionality in real-world applications. Performance evaluation methods and testing procedures are crucial steps in determining the sensor's sensitivity, linearity, durability, and response time. This evaluation process involves subjecting the strain sensor to controlled mechanical loading, environmental conditions, and calibration tests to assess its performance characteristics. By conducting comprehensive performance evaluations, researchers and engineers can validate the sensor's capabilities, optimize its design parameters, and enhance its overall performance for specific applications. This introduction sets the stage for understanding the importance of evaluating strain sensor performance and the methodologies involved in testing and validating their functionality. Fig. 7 shows the different types of equipment used for each characterization test. For example, the abrasion tester (Fig. 7a) is functional for washability test. The tensile machine (Fig. 7b) can be used for tensile test and stretching test of the strain sensor. The bending tester (Fig. 7c) can be used for evaluating the flexibility of strain sensors. Trypan blue assay (Fig. 7d) is one of the staining methods used in evaluating the biocompatibility of strain sensors.

The shape of strain sensors plays a critical role in determining their performance characteristics. Straight line designs offer
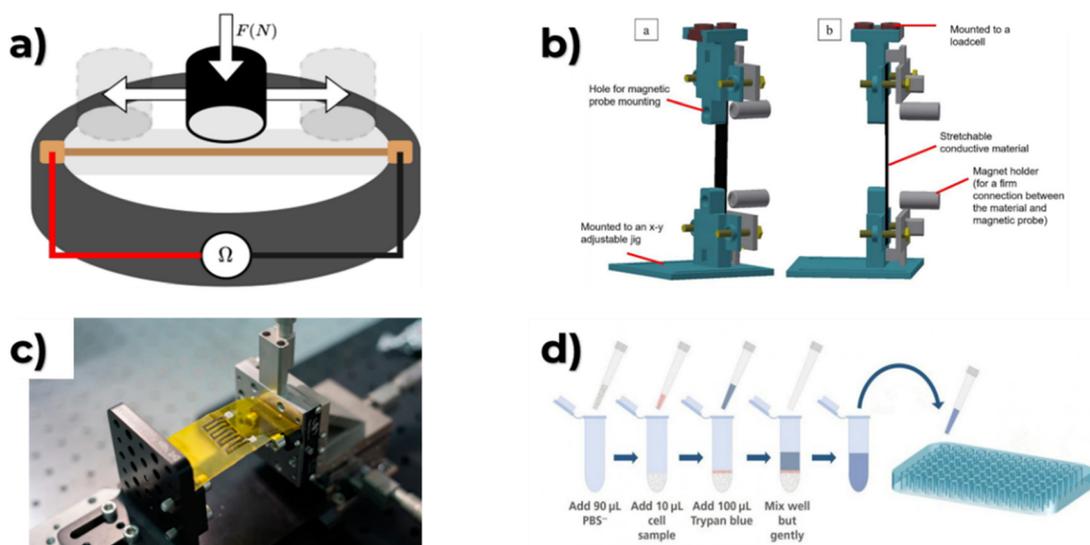

Fig. 7 Equipment for evaluating strain sensor performance. (a) Abrasion tester,[82] (b) tensile machine,[83] (c) electro-mechanical tester for bending test,[84] (d) trypan blue assay.[85]

simplicity and precision for basic strain measurements, while U-shapes provide a balance between flexibility and ease of fabrication. Serpentine patterns significantly enhance stretchability, making them ideal for wearable applications. Kirigami designs push the boundaries of flexibility and adaptability, allowing for extreme deformations. Each shape has its unique advantages, and the choice depends on the specific application requirements, highlighting the importance of tailored design in sensor development.

4.1. Washability test

The washability of strain sensors refers to their ability to withstand washing cycles without compromising their functionality or performance. Washable strain sensors are designed to maintain their sensing capabilities even after being subjected to washing processes, such as machine washing with conventional cleaning agents. This characteristic is crucial for strain sensors integrated into wearable technology, smart textiles, or garments, as it ensures that the sensors can be cleaned without deteriorating their sensing properties. Washable strain sensors are essential for applications where hygiene, durability, and long-term use are key factors.

A previous work[82] conducted an abrasion test on abraded copper-coated textile where an abrasion tester (Fig. 7a) was used from James Heal at 47.5 rpm with standard worsted wool and a constant pressure of 12 kPa for 60 000 cycles. Abrasion of the copper coating on the thread surface due to the wear from the abrasion test was observed.

A magnetic stirrer has also been used for washability analysis based on previous research.[86] The electronic textiles are subjected to a violent washing in a beaker with a magnetic stirrer at a rotation speed of 800 r min^{-1} for 3 min, which is much faster than the speed of a normal washing process. After that, the electronic textiles are dried in an oven at 60 °C for 12 h to finish one washing process. This process was repeated ten times, with the resistance and strain sensing performance of the e-textile strain sensor being tested after each washing and drying cycle. Another example of washability test that resulted in negligible change in resistance after repeated washing steps was reported.[87] Rigorous washability testing on thread-based strain sensors with different detergents was conducted. E-textile sensors are prone to various damage during washing, such as damage to conductive coatings, metallization layers, wires, conductive tracks, connections, protective layers, and textile changes. The evaluation of washability analysis helps in understanding the influence of different variables, including the textile substrate, conductive paste/ink, conductive yarns and textiles, protective coating, layout, design and integration, processing parameters, washing and drying parameters, and assessment criteria.

4.2. Linear test

The linear test is used to determine the sensitivity of a strain sensor by measuring the change in electrical resistance in response to a known and controlled amount of strain applied to the sensor. The sensitivity of a strain sensor is typically expressed as the gauge factor (GF), which is the ratio of the relative change in electrical resistance to the applied strain. In a linear stretching test, the GF is determined by applying a series of increasing strains to the sensor and measuring the corresponding changes in electrical resistance. The GF is then calculated as the slope of the linear relationship between the relative change in electrical resistance and the applied strain.

For example, a previous study[32] developed an ultrasensitive and stretchable strain sensor based on a conductive composite material. To verify the high sensitivity of the sensor, a linear stretching test was performed by applying a series of small strains to the sensor and measuring the corresponding changes in electrical resistance. A significant change in the resistance even under 1% strain was observed, indicating that the sensor had a high sensitivity to small strains.

4.3. Tensile test

A tensile test of a strain sensor involves subjecting the sensor to increasing amounts of strain to evaluate its stretchability and the maximum strain it can stretch. The stretchability of a strain sensor is related to its ability to maintain physical integrity and response stability under strain.[18] The tensile test can also measure the Young's modulus of the strain sensor using the stress/strain graph. The Young's modulus is a characteristic of the stretchable strain sensor that tells us how easily it can stretch and deform and is defined as the ratio of tensile stress (σ) to tensile strain (ε).

Previous research[88] has used tensile tests to determine the performance of various strain sensors. A crack-based strain sensor with high sensitivity and superior durability was developed for motion monitoring. The study used a tensile test to evaluate the sensor's performance, with the crack area proportion increasing rapidly from 16.9% to 48.8% as the tensile strain increased from 30% to 300%. The stretching and bending electromechanical behaviours of CCTSS were performed on an electronic universal tensile testing machine (UTM2203, Shenzhen Sun Technology Stock Co. Ltd) coupled with a digit precision multimeter (Tektronix, DMM 4050). An RST5200 electrochemical workstation (Suzhou Resitest Electronic Co., Ltd., China) was used to test the current (I)–voltage (V) relationship.

4.4. Cyclic test

A cyclic test for a strain sensor is a type of test used to evaluate the performance of the sensor under repeated loading and unloading cycles. The purpose of this test is to determine the sensor's ability to withstand repeated strain cycles without significant degradation in its performance. The test involves applying a cyclic strain to the sensor and measuring its response over a specified number of cycles. The cyclic strain can be applied in various ways, such as through the application of a cyclic load or a cyclic displacement.

It can be performed using various testing machines, such as a tensile testing machine or electromechanical tester. The testing machine can be programmed to apply a cyclic strain with a specific cycle, strain and time taken to read the electrical reading. The sensor's response can be measured using various techniques, such as resistance measurement, capacitance measurement, or optical measurement.

Previous research[89] has used cyclic stretching tests to determine the durability of strain sensors by evaluating their response to repeated stretching and releasing cycles. A developed practical strain sensor based on Ecoflex/graphene was tested for mechanical durability by applying strains of 15% and 40% to the sensor for 1000 cycles. The loading of tensile strain was performed using a universal testing machine (Shimadzu AGS-X), and the electrical signals of the strain sensor were recorded by a digital multimeter (GOGOL DM3068). The study found that the sensor maintained its response and stability throughout the cyclic tests, indicating its mechanical robustness and reliability.

Another study[90] conducted multi-cyclic stretching–releasing tests to assess the reproducibility, stability, durability, and reliability of the strain sensor for long-term use. The repeatability was measured by performing 100 stretching–releasing cyclic tests of the strain sensor at a tensile rate of 0.2 mm min^{-1} under a strain of 0.4%, 0.6%, 0.8% and 1%, respectively.

4.5. Signal latency test

The response and recovery time of a strain sensor refers to the time required for the sensor to reach a certain variation of resistance under a certain strain and to return to its original state. A study on a wearable strain sensor based on organohydrogel microsphere film reported a response and recovery time of 0.147 s when subjected to a 10% strain.[91] The less the response and recovery time, the better the sensor.

To evaluate the response time and relaxation time of a strain sensor, several evaluation methods can be used. One common method is to apply a strain to the sensor and measure the time it takes for the sensor to respond to the strain or until it reaches a stable state (Fig. 8). This can be done by applying an instantaneous tension to the sensor and measuring the time it takes for the sensor to reach a stable state. For example, in a study[92] on a fabric strain sensor, an instantaneous tension was applied to the sensor at a speed of 6 mm s^{-1} to a strain of 0.5%, and the response time was measured as the time it took for the sensor to reach a stable state.

4.6. Biocompatibility test

The biocompatibility of wearable strain sensors is an important consideration for their use in healthcare and biomedical applications. Thin film "plastic" strain sensors can be mounted closely on textile clothing or human skin comfortably to detect human activities without any harm to the human body.[93] A study assessed the biocompatibility of wearable C/TPU/Tegaderm strain sensors by conducting cell morphology and cell viability analysis, demonstrating their biocompatibility for use in healthcare applications.[94] The 100% cell viability indicated that the C/TPU/Tegaderm materials used are safe for application to human skin.

A previous study[31] performed the cytotoxicity test of hydrogels using U87-MG glioblastoma cells (ATCC HTB-14) cultured in Eagle's minimum essential medium (EMEM) with 10% fetal bovine serum (FBS) and 100 IU ml^{-1} penicillin and streptomycin and evaluated the cell viability using the trypan blue method. Another study[95] used human embryonic kidney cells (293FT cells) and human gastric epithelial cell line (GES1 cells) and the cell proliferation assay for the cytotoxicity test. Table 7 provides a list of methods that can be used to assess biocompatibility. The trypan blue method is a commonly used and widely accepted assay for assessing cell viability and has been shown to be effective in a variety of cell types, including HFF-1 cells. It is a relatively simple and quick assay that can provide qualitative information about the percentage of live and dead cells in a sample. In the context of a strain sensor experiment with HFF-1 cells, the trypan blue method may be a useful tool for assessing the cytotoxicity or biocompatibility of the sensor material. By comparing the percentage of live and dead cells in samples exposed to the sensor material to control samples, researchers can determine whether the material is causing damage to the cells and evaluate its safety for potential biomedical applications.

Rigorous testing methods are essential for assessing strain sensor performance. Techniques such as cyclic stretching, bending tests, stretch-to-failure tests, and washability assessments ensure that sensors meet the required standards for
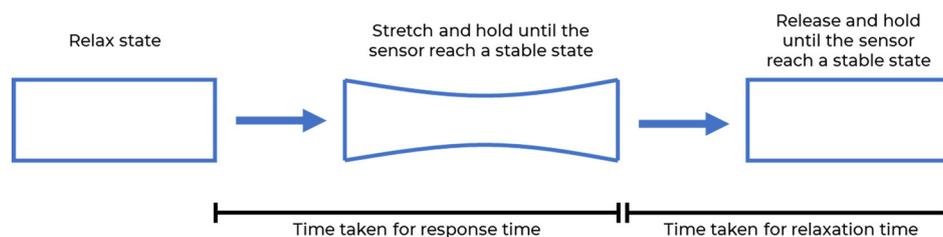
Fig. 8 Signal latency test.

Table 7 List of methods for biocompatibility assessment

Assay	Process	Advantage	Disadvantage	Ref.
Trypan blue	Distinguish between live and dead cells	• Simpler – requiring only a microscope and a dye solution • Can be performed in 5 to 10 min	Qualitative rather than a quantitative method	31 and 96
Cell proliferation	Measures the rate of cell division and growth	More specific to the process of cell division and can provide more detailed information about the growth rate and behaviour of cells	• Requires specialized equipment and reagents • Time-consuming – requires the cells to be seeded and allowed to grow and divide for a specific period before they can be quantified	95
MTT	Measures the metabolic activity of cells	Simple and easy to perform, requiring a microplate reader to measure the absorbance of the formazan product	Does not distinguish between live and dead cells	97

sensitivity, durability, and reliability in real-world applications. These evaluations are crucial for bridging the gap between laboratory prototypes and commercially viable products, highlighting the importance of standardized testing protocols in the field.

Conclusions

In conclusion, the development of strain sensors with high sensitivity, stretchability, durability, and biocompatibility is crucial for their application in various fields, including healthcare, sports, and robotics. This review paper has discussed the fabrication techniques, shape designs, and performance evaluation methods of strain sensors. Material selection plays a critical role in strain sensor performance, and various materials, such as carbon nanotubes, graphene, and polymer composites, have been explored for their fabrication. The strain sensor shape design, such as straight line, U-shape, serpentine, and kirigami, also significantly impacts their performance, and the appropriate shape design can enhance their sensitivity, stretchability, and durability. Performance evaluation methods, including washability, sensitivity, linearity, bending test, test till failure, stretchability, durability, response and recovery time, and biocompatibility, are essential to ensure the reliability and safety of strain sensors. This review is a valuable resource for researchers focusing on advancing the design of new strain sensors, setting quality benchmarks, optimizing sensor performance, and expanding the sensor potential applications.

Data availability

No primary research results, software or code have been included and no new data were generated or analysed as part of this review.

Author contributions

Conceptualization: Nur Nazihah Abu Hassan Zahri, Anis Nurashikin Nordin, Norsinnira Zainul Azlan. Methodology: Nur Nazihah Abu Hassan Zahri and Ibrahim Hafizu Hassan. Formal analysis: Nur Nazihah Abu Hassan Zahri, Anis Nurashikin

Nordin, Ibrahim Hafizu Hassan, Lun Hao Tung and Lai Ming Lim. Investigation: Nur Nazihah Abu Hassan Zahri and Anis Nurashikin Nordin. Resources: Lun Hao Tung and Lai Ming Lim. Writing – original draft: Nur Nazihah Abu Hassan Zahri. Writing – review & editing: Anis Nurashikin Nordin and Lun Hao Tung. Supervision: Anis Nurashikin Nordin, Lun Hao Tung and Lai Ming Lim. Project administration: Norsinnira Zainul Azlan and Anis Nurashikin Nordin. Funding acquisition: Norsinnira Zainul Azlan and Anis Nurashikin Nordin. All authors have read and agreed to the published version of the manuscript.

Conflicts of interest

There are no conflicts to declare.

Acknowledgements

References

1 S. Zhang, A. Chhetry, M. A. Zahed, S. Sharma, C. Park, S. Yoon and J. Y. Park, *npj Flexible Electron.*, 2022, **6**, 1–12.

2 Z. Zhao, Q. Li, Y. Dong, J. Gong, Z. Li, X. Qiao and J. Zhang, *Energy Technol.*, 2021, **9**, 1–13.

3 Y. He, M. Zhou, M. H. H. Mahmoud, X. Lu, G. He, L. Zhang, M. Huang, A. Y. Elnaggar, Q. Lei, H. Liu, C. Liu and I. H. E. Azab, *Adv. Compos. Hybrid Mater.*, 2022, **5**, 1939–1950.

4 T. N. Nguyen, S. Chun and J. Kim, *J. Ind. Text.*, 2023, **53**, 1–17.

5 W. Geng, T. J. Cuthbert and C. Menon, *ACS Appl. Polym. Mater.*, 2021, **3**, 122–129.

6 L. Wang, T. Xu, C. Fan and X. Zhang, *iScience*, 2021, **24**, 102028.

7 Y. G. Kim, J. H. Song, S. Hong and S. H. Ahn, *npj Flexible Electron.*, 2022, **6**, 1–8.

8 Z. Pei, Q. Zhang, K. Yang, Z. Yuan, W. Zhang and S. Sang, *Adv. Mater. Technol.*, 2021, **6**, 1–7, DOI: 10.1002/ADMT.202100038.

9 V. Sencadas, R. Mutlu and G. Alici, *Sens. Actuators, A*, 2017, **266**, 56–64.

10 C. Tang, M. Xu, W. Yi, Z. Zhang, E. Occhipinti, C. Dong, D. Ravenscroft, S. M. Jung, S. Lee, S. Gao, J. M. Kim and L. G. Occhipinti, *npj Flexible Electron.*, 2024, **8**, 1–11.

11 W. Tang, T. Yan, F. Wang, J. Yang, J. Wu, J. Wang, T. Yue and Z. Li, *Carbon*, 2019, **147**, 295–302.

12 D. Zhang, Y. Tang, Y. Zhang, F. Yang, Y. Liu, X. Wang, J. Yang, X. Gong and J. Zheng, *J. Mater. Chem. A*, 2020, **8**, 20474–20485.

13 C. Yang, J. Yin, Z. Chen, H. Du, M. Tian, M. Zhang, J. Zheng, L. Ding, P. Zhang, X. Zhang and K. Deng, *Macromol. Mater. Eng.*, 2020, **305**, 2000479.

14 Q. Zhang, L. Liu, D. Zhao, Q. Duan, J. Ji, A. Jian, W. Zhang and S. Sang, *Nanomaterials*, 2017, **7**(12), 424.

15 W. Zhai, J. Zhu, Z. Wang, Y. Zhao, P. Zhan, S. Wang, G. Zheng, C. Shao, K. Dai, C. Liu and C. Shen, *ACS Appl. Mater. Interfaces*, 2022, **14**, 4562–4570.

16 X. Liao, Z. Zhang, Z. Kang, F. Gao, Q. Liao and Y. Zhang, *Mater. Horiz.*, 2017, **4**, 502–510.

17 H. Souri and D. Bhattacharyya, *Sens. Actuators, A*, 2019, **285**, 142–148.

18 H. Souri, H. Banerjee, A. Jusufi, N. Radacsi, A. A. Stokes, I. Park, M. Sitti and M. Amjadi, *Adv. Intell. Syst.*, 2020, **2**, 2000039.

19 N. Afsarimanesh, A. Nag, S. Sarkar, G. S. Sabet, T. Han and S. C. Mukhopadhyay, *Sens. Actuators, A*, 2020, **315**, 112355.

20 Y. Liu, H. Wang, W. Zhao, M. Zhang, H. Qin and Y. Xie, *Sensors*, 2018, **18**, 645.

21 N. Zavanelli, K. Kwon and W. H. Yeo, *IEEE Open J. Eng. Med. Biol.*, 2023, 1–35.

22 Y. Si, S. Chen, M. Li, S. Li, Y. Pei and X. Guo, *Adv. Intell. Syst.*, 2022, **4**, 2100046.

23 S. Wu, S. Peng, Y. Yu and C. H. Wang, *Adv. Mater. Technol.*, 2020, **5**(2), 1900908.

24 L. Duan, D. R. D'hooge and L. Cardon, *Prog. Mater. Sci.*, 2020, **114**, 100617.

25 A. Qiu, P. Li, Z. Yang, Y. Yao, I. Lee and J. Ma, *Adv. Funct. Mater.*, 2019, **29**, 1806306.

26 A. Yadav, N. Yadav, Y. Wu, S. RamaKrishna and Z. Hongyu, *Mater. Adv.*, 2023, **4**, 1444–1459.

27 H. Wang, J. Liu, H. Cui, Y. Liu, J. Zhu, H. Wang, G. Song, Z. Li and D. Chen, *ACS Appl. Electron. Mater.*, 2021, **3**, 1758–1770.

28 P. Liu, W. Pan, Y. Liu, J. Liu, W. Xu, X. Guo, C. Liu, Y. Zhang, Y. Ge and Y. Huang, *Compos. Sci. Technol.*, 2018, **159**, 42–49.

29 Y. Hu, T. Zhao, P. Zhu, Y. Zhang, X. Liang, R. Sun and C.-P. Wong, *Nano Res.*, 2018, **11**, 1938–1955.

30 H. Souri and D. Bhattacharyya, *Mater. Des.*, 2018, **154**, 217–227.

31 J. Wang, Y. Liu, S. Su, J. Wei, S. E. Rahman, F. Ning, G. Christopher, W. Cong and J. Qiu, *Polymer*, 2019, **11**, 1873.

32 H. Sun, X. Fang, Z. Fang, L. Zhao, B. Tian, P. Verma, R. Maeda and Z. Jiang, *Microsyst. Nanoeng.*, 2022, **8**, 1–10.

33 W. C. Gao, W. Wu, C. Z. Chen, H. Zhao, Y. Liu, Q. Li, C. X. Huang, G. H. Hu, S. F. Wang, D. Shi and Q. C. Zhang, *ACS Appl. Mater. Interfaces*, 2022, **14**, 1874–1884.

34 J. Yang, K. Ling, L. Liu, X. Zeng, X. Xu, Z. Li and P. He, *IEEE Sens. J.*, 2022, **22**, 13937–13944.

35 M. Qu, Y. Qin, Y. Sun, H. Xu, D. W. Schubert, K. Zheng, W. Xu and F. Nilsson, *ACS Appl. Mater. Interfaces*, 2020, **12**, 42140–42152.

36 R. Wang, W. Xu, W. Shen, X. Shi, J. Huang and W. Song, *Inorg. Chem. Front.*, 2019, **6**, 3119–3124.

37 X. Fu, M. Ramos, A. M. Al-Jumaily, A. Meshkinzar and X. Huang, *J. Mater. Sci.*, 2019, **54**, 2170–2180.

38 M. Amjadi, Y. J. Yoon and I. Park, *Nanotechnology*, 2015, **26**, 375501.

39 A. Qiu, M. Aakyiir, R. Wang, Z. Yang, A. Umer, I. Lee, H. Y. Hsu and J. Ma, *Mater. Adv.*, 2020, **1**, 235–243.

40 K. Xu, Y. Lu, S. Honda, T. Arie, S. Akita and K. Takei, *J. Mater. Chem. C*, 2019, **7**, 9609–9617.

41 J. T. Muth, D. M. Vogt, R. L. Truby, I. Mengüç, D. B. Kolesky, R. J. Wood, J. A. Lewis, J. T. Muth, R. L. Truby, D. B. Kolesky, J. A. Lewis, D. M. Vogt, Y. Mengüç and R. J. Wood, *Adv. Mater.*, 2014, **26**(36), 6307–6312.

42 Y. Li, Y. A. Samad, T. Taha, G. Cai, S. Y. Fu and K. Liao, *ACS Sustainable Chem. Eng.*, 2016, **4**, 4288–4295.

43 H. Liu, H. Jiang, F. Du, D. Zhang, Z. Li and H. Zhou, *ACS Sustainable Chem. Eng.*, 2017, **5**, 10538–10543.

44 S. Wang, H. Cheng, B. Yao, H. He, L. Zhang, S. Yue, Z. Wang and J. Ouyang, *ACS Appl. Mater. Interfaces*, 2021, **13**, 20735–20745.

45 S. Azadi, S. Peng, S. A. Moshizi, M. Asadnia, J. Xu, I. Park, C. H. Wang and S. Wu, *Adv. Mater. Technol.*, 2020, **5**(11), 2000426.

46 Y. Cai, J. Qin, W. Li, A. Tyagi, Z. Liu, M. D. Hossain, H. Chen, J. K. Kim, H. Liu, M. Zhuang, J. You, F. Xu, X. Lu, D. Sun and Z. Luo, *J. Mater. Chem. A*, 2019, **7**, 27099–27109.

47 H. Xu, Y. Lv, D. Qiu, Y. Zhou, H. Zeng and Y. Chu, *Nanoscale*, 2019, **11**, 1570–1578.

48 N. A. Demidenko, A. V. Kuksin, V. V. Molodykh, E. S. Pyankov, L. P. Ichkitidze, V. A. Zaborova, A. A. Tsymbal, S. A. Tkachenko, H. Shafaei, E. Diachkova and A. Y. Gerasimenko, *Bioengineering*, 2022, **9**(1), 9010036.

49 Y. Cai, J. Qin, W. Li, A. Tyagi, Z. Liu, M. D. Hossain, H. Chen, J. K. Kim, H. Liu, M. Zhuang, J. You, F. Xu, X. Lu, D. Sun and Z. Luo, *J. Mater. Chem. A*, 2019, **7**, 27099–27109.

50 S. H. Ke, P. W. Guo, C. Y. Pang, B. Tian, C. S. Luo, H. P. Zhu and W. Wu, *Adv. Mater. Technol.*, 2020, **5**(5), 1901097.

51 I. Ertugrul, O. Ulkir, S. Ersoy and M. Ragulskis, *Polymers*, 2023, **15**(4), 0991.

52 N. H. M. Mustapha, M. R. M. Razif, S. H. Nasir, I. N. A. M. Nordin and Y. T. Mi, *Jurnal Teknologi*, 2023, **85**(4), 27–35.

53 E. Kantarak, S. Rucman, T. Kumpika, W. Sroila, P. Tippo, A. Panthawan, P. Sanmuangmoon, A. Sriboonruang, N. Jhuntama, O. Wiranwetchayan, W. Thongsuwan and P. Singjai, *Appl. Compos. Mater.*, 2020, **27**, 955–968.

54 S. H. Ke, P. W. Guo, C. Y. Pang, B. Tian, C. S. Luo, H. P. Zhu and W. Wu, *Adv. Mater. Technol.*, 2020, **5**(5), 1901097, DOI: **10.1002/ADMT.201901097**.

55 X. Gong, K. Huang, Y. H. Wu and X. S. Zhang, *Sens. Actuators, A*, 2022, **345**, 113821.

56 X. Qi, H. Ha, B. Hwang and S. Lim, *Appl. Sci.*, 2020, **10**, 6983.

57 N. Anderson, N. Szorc, V. Gunasekaran, S. Joshi and G. Jursich, *Sens. Actuators, A*, 2019, **290**, 1–7.

58 X. Yang, J. Gui, C. Dong, J. Zhao and R. Xu, *ACS Appl. Nano Mater.*, 2023, **6**, 21679–21687.

59 X. Yang, J. Gui, C. Dong, J. Zhao and R. Xu, *ACS Appl. Nano Mater.*, 2023, **6**, 21679–21687.

60 H. Jeong and S. Lim, *Sensors*, 2016, **16**, 1839.

61 N. Anderson, N. Szorc, V. Gunasekaran, S. Joshi and G. Jursich, *Sens. Actuators, A*, 2019, **290**, 1–7.

62 T. Han, S. Kundu, A. Nag and Y. Xu, *Sensors*, 2019, **19**(7), 1706, DOI: **10.3390/S19071706**.

63 A. Coste, L. Oliveira Da Fonseca, J. Guillermo, C. Alfaro and A. L. Trejos, *Sensors*, 2023, **23**, 1503.

64 Y. Xia, Q. Zhang, X. E. Wu, T. V. Kirk and X. D. Chen, *Sensors*, 2019, **19**, 4553.

65 X. Li, K. H. Koh, M. Farhan and K. W. C. Lai, *Nanoscale*, 2020, **12**, 4110–4118.

66 W. Lu, B. Mustafa, Z. Wang, F. Lian and G. Yu, *Nanomaterials*, 2022, **12**(5), 871, DOI: **10.3390/NANO12050871/S1**.

67 Y. Zhao, M. Ren, Y. Shang, J. Li, S. Wang, W. Zhai, G. Zheng, K. Dai, C. Liu and C. Shen, *Compos. Sci. Technol.*, 2020, **200**, 108448.

68 E. Aslanidis, E. Skotadis, E. Moutoulas and D. Tsoukalas, *Sensors*, 2020, **20**(9), 2584.

69 F. Fang, H. Wang, H. Wang, X. Gu, J. Zeng, Z. Wang, X. Chen, X. Chen and M. Chen, *Micromachines*, 2021, **12**, 252.

70 Y. X. Song, W. M. Xu, M. Z. Rong and M. Q. Zhang, *J. Mater. Chem. A*, 2019, **7**, 2315–2325.

71 R. Madhavan, *J. Mater. Sci.: Mater. Electron.*, 2022, **33**, 3465–3484.

72 A. Qiu, M. Aakyiir, R. Wang, Z. Yang, A. Umer, I. Lee, H. Y. Hsu and J. Ma, *Mater. Adv.*, 2020, **1**, 235–243.

73 J. Zhou, X. Guo, Z. Xu, Q. Wu, J. Chen, J. Wu, Y. Dai, L. Qu and Z. Huang, *Compos. Sci. Technol.*, 2020, **197**, 108215.

74 C. Yan, J. Wang, W. Kang, M. Cui, X. Wang, C. Y. Foo, K. J. Chee and P. S. Lee, *Adv. Mater.*, 2014, **26**, 2022–2027.

75 K. Yong, S. De, E. Y. Hsieh, J. Leem, N. R. Aluru and S. W. Nam, *Mater. Today*, 2020, **34**, 58–65.

76 S. Li, G. Liu, R. Li, Q. Li, Y. Zhao, M. Huang, M. Zhang, S. Yin, Y. Zhou, H. Tang, L. Wang, G. Fang and Y. Su, *ACS Nano*, 2022, **16**, 541–553.

77 S. Hossen, A. N. Nordin, M. I. Suhaimi, L. L. Ming, N. Z. Azlan, R. A. Rahim, M. S. Riza and Z. Samsudin, *IFMBE Proceedings*, 2024, vol. 107, pp. 65–72.

78 J. Zhou, X. Guo, Z. Xu, Q. Wu, J. Chen, J. Wu, Y. Dai, L. Qu and Z. Huang, *Compos. Sci. Technol.*, 2020, **197**, 108215, DOI: **10.1016/J.COMPSCITECH.2020.108215**.

79 O. A. Araromi, M. A. Graule, K. L. Dorsey, S. Castellanos, J. R. Foster, W. H. Hsu, A. E. Passy, J. J. Vlassak, J. C. Weaver, C. J. Walsh and R. J. Wood, *Nature*, 2020, **587**(7833), 219–224.

80 Y. T. Huang, S. C. Huang, C. C. Hsu, R. M. Chao and T. K. Vu, *Sensors*, 2012, **12**, 3269–3280.

81 K. Yong, S. De, E. Y. Hsieh, J. Leem, N. R. Aluru and S. Nam, *Mater. Today*, 2020, **34**, 58–65.

82 P. Petz, C. Biermaier, J. Scharinger and J. Langer, *Conference Record - IEEE Instrumentation and Measurement Technology Conference*, 2023, p. 10175942.

83 A. Wiranata, Y. Ohsugi, A. Minaminosono, Y. Kuwajima and S. Maeda, *HardwareX*, 2022, **11**, e00287.

84 R. Feng, Y. Mu, X. Zeng, W. Jia, Y. Liu, X. Jiang, Q. Gong and Y. Hu, *Sensors*, 2021, **21**, 3969.

85 Trypan Blue Staining Protocol|Creative Bioarray, **https://www.creative-bioarray.com/support/trypan-blue-staining-assay.htm**, (accessed 16 April 2024).

86 T. Sun, Y. D. Jiang, Z. H. Duan, Z. Yuan, Y. Wang and H. L. Tai, *Sci. China: Technol. Sci.*, 2021, **64**, 441–450.

87 A. Sadeqi, H. Rezaei Nejad, F. Alaimo, H. Yun, M. Punjiya and S. R. Sonkusale, *IEEE Sens. J.*, 2018, **18**, 9137–9144.

88 Y. Zhou, P. Zhan, M. Ren, G. Zheng, K. Dai, L. Mi, C. Liu and C. Shen, *ACS Appl. Mater. Interfaces*, 2019, **11**, 7405–7414.

89 Y. Fan, H. Zhao, Y. Yang, Y. Yang, T. Ren and H. Tu, *Front. Sens.*, 2022, **2**, 815209.

90 Y. Zheng, Y. Li, Y. Zhou, K. Dai, G. Zheng, B. Zhang, C. Liu and C. Shen, *ACS Appl. Mater. Interfaces*, 2020, **12**, 1474–1485.

91 K. Zhai, H. Wang, Q. Ding, Z. Wu, M. Ding, K. Tao, B. R. Yang, X. Xie, C. Li and J. Wu, *Adv. Sci.*, 2022, **10**(6), 5632, DOI: **10.1002/ADVS.202205632**.

92 X. Chen, F. Wang, L. Shu, X. Tao, L. Wei, X. Xu, Q. Zeng and G. Huang, *Mater. Des.*, 2022, **221**, 110926.

93 X. Fan, N. Wang, J. Wang, B. Xu and F. Yan, *Mater. Chem. Front.*, 2018, **2**, 355–361.

94 N. N. A. H. Zahri, A. N. Nordin, A. F. M. Mansor, R. A. Rahim, A. A. M. Ralib, M. I. Suhaimi and L. L. Ming, *9th International Conference on Computer and Communication Engineering (ICCCE)*, 2023, pp. 173–176, DOI: **10.1109/ICCCE58854.2023.10246041**.

95 C. Tan, Z. Dong, Y. Li, H. Zhao, X. Huang, Z. Zhou, J. W. Jiang, Y. Z. Long, P. Jiang, T. Y. Zhang and B. Sun, *Nat. Commun.*, 2020, **11**, 1–10.

96 W. Strober, *Curr. Protoc. Immunol.*, 2015, **111**, A3.B.1.

97 M. Salari, S. Mohseni Taromsari, R. Bagheri and M. A. Faghihi Sani, *J. Mater. Sci.*, 2019, **54**, 4259–4276.